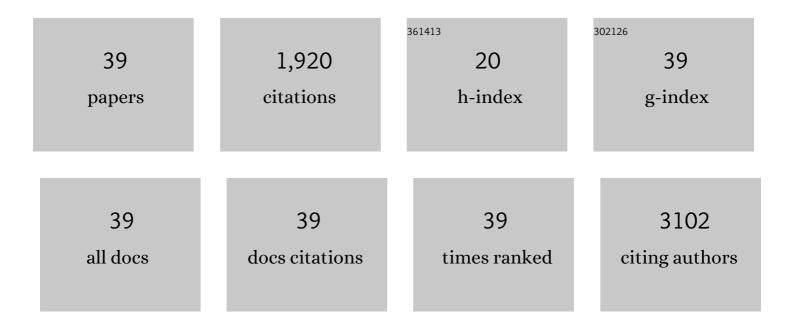
## Susan M Noworolski

List of Publications by Year in descending order

Source: https://exaly.com/author-pdf/7951484/publications.pdf Version: 2024-02-01



#	Article	IF	CITATIONS
1	Identification of prostate cancer using multiparametric MR imaging characteristics of prostate tissues referenced to whole mount histopathology. Magnetic Resonance Imaging, 2022, 85, 251-261.	1.8	7
2	Effects of Isocaloric Fructose Restriction on Ceramide Levels in Children with Obesity and Cardiometabolic Risk: Relation to Hepatic De Novo Lipogenesis and Insulin Sensitivity. Nutrients, 2022, 14, 1432.	4.1	8
3	Assessing highâ€intensity focused ultrasound treatment of prostate cancer with hyperpolarized <sup>13</sup> C dualâ€agent imaging of metabolism and perfusion. NMR in Biomedicine, 2019, 32, e3962.	2.8	10
4	Isocaloric Fructose Restriction Reduces Serum d-Lactate Concentration in Children With Obesity and Metabolic Syndrome. Journal of Clinical Endocrinology and Metabolism, 2019, 104, 3003-3011.	3.6	14
5	Quantitative imaging biomarkers alliance (QIBA) recommendations for improved precision of DWI and DCEâ€MRI derived biomarkers in multicenter oncology trials. Journal of Magnetic Resonance Imaging, 2019, 49, i.	3.4	5
6	Quantitative imaging biomarkers alliance (QIBA) recommendations for improved precision of DWI and DCEâ€MRI derived biomarkers in multicenter oncology trials. Journal of Magnetic Resonance Imaging, 2019, 49, e101-e121.	3.4	241
7	Phase I Study of CTT1057, an 18F-Labeled Imaging Agent with Phosphoramidate Core Targeting Prostate-Specific Membrane Antigen in Prostate Cancer. Journal of Nuclear Medicine, 2019, 60, 910-916.	5.0	35
8	Phase I study of dose escalation to dominant intraprostatic lesions using high-dose-rate brachytherapy. Journal of Contemporary Brachytherapy, 2018, 10, 193-201.	0.9	12
9	Improved multiparametric MRI discrimination between lowâ€risk prostate cancer and benign tissues in a small cohort of 5αâ€reductase inhibitor treated individuals as compared with an untreated cohort. NMR in Biomedicine, 2017, 30, e3696.	2.8	11
10	Effects of Dietary Fructose Restriction on Liver Fat, De Novo Lipogenesis, and Insulin Kinetics in Children With Obesity. Gastroenterology, 2017, 153, 743-752.	1.3	189
11	Human immunodeficiency virus–infected and uninfected adults with non–genotype 3 hepatitis C virus have less hepatic steatosis than adults with neither infection. Hepatology, 2017, 65, 853-863.	7.3	25
12	Characterization and stratification of prostate lesions based on comprehensive multiparametric MRI using detailed wholeâ€mount histopathology as a reference standard. NMR in Biomedicine, 2017, 30, e3796.	2.8	19
13	Controlled attenuation parameter and magnetic resonance spectroscopy-measured liver steatosis are discordant in obese HIV-infected adults. Aids, 2017, 31, 2119-2125.	2.2	18
14	18F Fluorocholine Dynamic Time-of-Flight PET/MR Imaging in Patients with Newly Diagnosed Intermediate- to High-Risk Prostate Cancer: Initial Clinical-Pathologic Comparisons. Radiology, 2017, 282, 429-436.	7.3	15
15	Isocaloric fructose restriction and metabolic improvement in children with obesity and metabolic syndrome. Obesity, 2016, 24, 453-460.	3.0	145
16	Short-term isocaloric fructose restriction lowers apoC-III levels and yields less atherogenic lipoprotein profiles in children with obesity and metabolic syndrome. Atherosclerosis, 2016, 253, 171-177.	0.8	42
17	Practical aspects of prostate MRI: hardware and software considerations, protocols, and patient preparation. Abdominal Radiology, 2016, 41, 817-830.	2.1	12
18	High-Resolution 3-T Endorectal Prostate MRI: A Multireader Study of Radiologist Preference and Perceived Interpretive Quality of 2D and 3D T2-Weighted Fast Spin-Echo MR Images. American Journal of Roentgenology, 2016, 206, 86-91.	2.2	25

#	Article	IF	CITATIONS
19	Effect of a High-Fructose Weight-Maintaining Diet on Lipogenesis and Liver Fat. Journal of Clinical Endocrinology and Metabolism, 2015, 100, 2434-2442.	3.6	180
20	Reduced-FOV excitation decreases susceptibility artifact in diffusion-weighted MRI with endorectal coil for prostate cancer detection. Magnetic Resonance Imaging, 2015, 33, 56-62.	1.8	86
21	Bone Structure and Perfusion Quantification of Bone Marrow Edema Pattern in the Wrist of Patients with Rheumatoid Arthritis: A Multimodality Study. Journal of Rheumatology, 2014, 41, 1766-1773.	2.0	14
22	Semiautomatic registration of digital histopathology images to in vivo MR images in molded and unmolded prostates. Journal of Magnetic Resonance Imaging, 2014, 39, 1223-1229.	3.4	3
23	Abnormal findings on multiparametric prostate magnetic resonance imaging predict subsequent biopsy upgrade in patients with low risk prostate cancer managed with active surveillance. Abdominal Imaging, 2014, 39, 1027-1035.	2.0	12
24	A Randomized Controlled Trial of a Mindfulness-Based Intervention for Metabolic Health in Obese Adults. Journal of Alternative and Complementary Medicine, 2014, 20, A15-A15.	2.1	1
25	Role of endorectal MR imaging and MR spectroscopic imaging in defining treatable intraprostatic tumor foci in prostate cancer: Quantitative analysis of imaging contour compared to whole-mount histopathology. Radiotherapy and Oncology, 2014, 110, 303-308.	0.6	39
26	Liver Steatosis: Concordance of MR Imaging and MR Spectroscopic Data with Histologic Grade. Radiology, 2012, 264, 88-96.	7.3	37
27	Liver diffusivity in healthy volunteers and patients with chronic liver disease: Comparison of breathhold and freeâ€breathing techniques. Journal of Magnetic Resonance Imaging, 2012, 35, 103-109.	3.4	9
28	Quantitative characterization of bone marrow edema pattern in rheumatoid arthritis using 3 tesla MRI. Journal of Magnetic Resonance Imaging, 2012, 35, 211-217.	3.4	28
29	Clinical Investigations Interactive, multi-modality image registrations for combined MRI/MRSI-planned HDR prostate brachytherapy. Journal of Contemporary Brachytherapy, 2011, 1, 26-31.	0.9	7
30	A pilot study of endorectal magnetic resonance imaging and magnetic resonance spectroscopic imaging changes with dutasteride in patients with low risk prostate cancer. BJU International, 2011, 108, E164-E170.	2.5	8
31	Postâ€processing correction of the endorectal coil reception effects in MR spectroscopic imaging of the prostate. Journal of Magnetic Resonance Imaging, 2010, 32, 654-662.	3.4	17
32	Magnetic resonance imaging for secondary assessment of breast density in a high-risk cohort. Magnetic Resonance Imaging, 2010, 28, 8-15.	1.8	111
33	Respiratory motion-corrected proton magnetic resonance spectroscopy of the liver. Magnetic Resonance Imaging, 2009, 27, 570-576.	1.8	26
34	A clinical comparison of rigid and inflatable endorectal oil probes for MRI and 3D MR spectroscopic imaging (MRSI) of the prostate. Journal of Magnetic Resonance Imaging, 2008, 27, 1077-1082.	3.4	30
35	Liver Steatosis: Investigation of Opposed-Phase T1-weighted Liver MR Signal Intensity Loss and Visceral Fat Measurement as Biomarkers. Radiology, 2008, 249, 160-166.	7.3	51
36	Assessment of metastatic cervical adenopathy using dynamic contrast-enhanced MR imaging. American Journal of Neuroradiology, 2003, 24, 301-11.	2.4	91

#	Article	IF	CITATIONS
37	Time-dependent effects of hormone-deprivation therapy on prostate metabolism as detected by combined magnetic resonance imaging and 3D magnetic resonance spectroscopic imaging. Magnetic Resonance in Medicine, 2001, 46, 49-57.	3.0	120
38	An automated technique for the quantitative assessment of 3D-MRSI data from patients with glioma. Journal of Magnetic Resonance Imaging, 2001, 13, 167-177.	3.4	135
39	High spatial resolution1H-MRSI and segmented MRI of cortical gray matter and subcortical white matter in three regions of the human brain. Magnetic Resonance in Medicine, 1999, 41, 21-29.	3.0	82